

Preparation and characterization of a novel electrospun ammonium molybdophosphate/polyacrylonitrile nanofiber adsorbent for cesium removal

Amin Tabatabaefar · Ali Reza Keshtkar ·
Mohammad Ali Moosavian

Received: 24 December 2014 / Published online: 14 February 2015
© Akadémiai Kiadó, Budapest, Hungary 2015

Abstract Adsorption of Cs^+ ion from aqueous solution onto a novel electrospun ammonium molybdophosphate/polyacrylonitrile nanofiber adsorbent with variation in AMP content, adsorbent concentration, pH, contact time, initial concentration and temperature was studied. The physicochemical characterization was performed by FTIR, XRD, BET and SEM analyses. Langmuir, Freundlich and Dubinin–Radushkevich models were used for analysis of equilibrium data. Kinetic results showed that the experimental data best fitted the pseudo-second-order kinetic model. The adsorption affinity of metal ions onto adsorbent was in order of $\text{Cs}^+ > \text{Co}^{2+} > \text{Mg}^{2+} > \text{Ca}^{2+} > \text{Sr}^{2+}$. The adsorbent could be easily regenerated after five cycles of adsorption–desorption.

Keywords Adsorption · Cesium · AMP/PAN · Electrospun · Nanofiber

Introduction

In recent years, researchers have been seriously concerned with the issue of toxic effects of heavy metals pollution on the environment especially in bodies of water [1, 2]. Cesium metal which is originated from nuclear waste is kind of long-lived heavy metals that are presented in the environment [3]. Also, some of this pollution is related to industries such as fiber optic, telecommunication systems, night-vision

equipment and catalysts that use cesium compounds for their special physicochemical properties [4]. Environmental pollution is arisen from wastewater containing toxic substances such as Cs^+ during the enhancing industrial activities. Cs^+ has been a topic of serious concern for long half-life and high water solubility. Therefore, it can be easily adsorbed by marine animals and directly come to human food chains [5]. The effective removal of toxic substances needs constant improvement/upgrading of processes and technologies for treatment [6, 7].

Various technologies have been investigated for the removal of toxic metals from industrial wastewater such as thermal treatment, precipitation, reverse osmosis, membrane filtration, solvent extraction, biological treatment and inorganic and organic ion exchange processes [8–10]. Most of these methods are limited by technical, economic, environmental and health problems that correspond to low efficiency, long-time of processing and high-energy consumption. Adsorption is a relatively mature and attractive method because of its high efficiency, ease of handling and the availability of different adsorbents that are applied to eliminate ions from aqueous solutions [11, 12]. Recently, different adsorbents were used for Cs^+ removal from aqueous solutions using prussian blue caged in alginate/calcium beads [13], potassium hexacyanocobalt ferrate [14], ammonium molybdophosphate–calcium alginate composite [15] and polyacrylonitrile based manganese dioxide composite [16]. Among the previous adsorbents, combination of ammonium molybdophosphate–polyacrylonitrile (AMP–PAN) in the form of granule composite prepared by Sebesta [17] and later developed by Park et al. [18] had effective properties of removing Cs^+ that reached the maximum adsorption capacity of 0.61 mmol Cs^+ /g adsorbent.

Nanofiber technology is one of the most major issues in the recent research topics. Electrospinning is a simple,

A. Tabatabaefar · M. A. Moosavian
Department of Chemical Engineering, Faculty of Engineering,
University of Tehran, Tehran, Iran

A. R. Keshtkar (✉)
Nuclear Fuel Cycle School, Nuclear Science and Technology
Research Institute, Tehran, Iran
e-mail: akeshkar@aeoi.org.ir

convenient, effective and widely utilized method for generation of nanofibers ranging from 50 to 500 nm in diameter. It appropriately allows the preparation of nanofibers with interesting characteristics such as thin diameters, large surface area per unit mass, high porosity and interfibrous pore size [19–21]. In the electrospinning technique, high voltage is used between a needle and a collector. An electrically charged jet of composite solution is created during the process. The solvent vaporizes before reaching the collector and the fibers with micro or nano-sized diameters collect on a collector. The parameters which influence electrospinning involve composite solution properties, process and ambient conditions [22].

In this study, a novel AMP–PAN nanofiber adsorbent which was prepared by the electrospinning technique has been utilized for Cs^+ ion removal from aqueous solution. The adsorbent was characterized by Fourier transform infrared spectroscopy (FTIR), Brunauer–Emmett–Teller (BET), X-ray powder diffraction (XRD) and scanning electron microscopy (SEM) analyses. The influences of AMP content, adsorbent concentration, pH, contact time, initial Cs^+ ion concentration and temperature were investigated on the removal of Cs^+ from aqueous solution by AMP/PAN nanofiber adsorbent. Also, the adsorbent capability for adsorption of Co^{2+} , Sr^{2+} , Mg^{2+} and Ca^{2+} ions was investigated. Moreover, the well-known isotherm and kinetic models were applied to the experimental data. Also, thermodynamic parameters of Cs^+ adsorption process were evaluated and finally, the reusability of the AMP/PAN nanofiber adsorbent was determined.

Experimental

Chemicals and reagent

Ammonium phosphomolybdate hydrate $[(\text{NH}_4)_3\text{PMo}_{12}\text{O}_{40} \cdot x\text{H}_2\text{O}]$, polyacrylonitrile (MW = 150,000) and dimethyl sulfoxide [DMSO, $(\text{CH}_3)_2\text{SO}$, 99.5 %] were used to synthesize AMP/PAN. Polysorbate 80 (TWEEN 80, Panreac, viscosity 300–500 cSt) was applied as a surfactant model. The stock solutions of Cs^+ , Co^{2+} , Sr^{2+} , Ca^{2+} and Mg^{2+} were prepared by dissolving weighed amount of CsCl , $\text{CoCl}_2 \cdot 6\text{H}_2\text{O}$, $\text{SrCl}_2 \cdot 6\text{H}_2\text{O}$, $\text{CaCl}_2 \cdot 2\text{H}_2\text{O}$ and $\text{MgCl}_2 \cdot 6\text{H}_2\text{O}$ in deionized water, respectively. All reagents were provided from Sigma–Aldrich and Merck and were used without further purification.

Preparation of AMP/PAN nanofiber

For preparation of AMP/PAN nanofiber with different weight percentages (wt%) of AMP (17, 43 and 46) based on the composite weight, first 10 mL of DMSO and 0.7 g

of PAN were mixed at 50 °C and 250 rpm using mechanical agitator for 1 h. Then, 0.140, 0.525 and 0.595 g of AMP with one drop of TWEEN 80 were added to the previous homogenous solution and stirred at 50 °C and 250 rpm for 5 h. The prepared green homogenous solution as a composite was used for electrospinning. The prepared homogeneous solutions were put into 10 mL plastic syringe with a 0.5 mm diameter capillary tip. A variable high voltage generator was utilized for the electrospinning process. The negative terminal was connected to an aluminum foil and the positive terminal of a high voltage generator was connected to the metallic syringe head. The used voltage was 20 kV. The electrospun fibers were collected on an aluminum foil coiled on a metal cylinder rotating at 200 rpm. The flow rate of the spinning solution was 1 mL/h and the distance between the syringe tip and the collector was 80 mm.

Adsorption experiments

All adsorption experiments were carried out using batch method by adding 0.05 g of adsorbent to 50 mL of Cs^+ solution on a rotary with an initial concentration of 100 mg/L at 150 rpm. The effect of pH on Cs^+ adsorption was investigated in the range of 1–6. The initial pH of solution was adjusted with 0.1 M NaOH and 0.1 M HCl. In order to study kinetics, the experiments were performed at pH 5. To obtain adsorption isotherms, various initial concentrations were used (10–100 mg/L) at pH 5 and different temperatures (25–45 °C). The equilibrium adsorption experiments for other metal ions including Co^{2+} , Sr^{2+} , Mg^{2+} and Ca^{2+} ions were performed in single component systems by adding 0.05 g of the adsorbent to 50 mL of each individual metal ion solution with an initial concentration of 100 mg/L at pH 5. The aqueous phase concentration of Cs^+ and other metal ions were distinguished by atomic absorption spectroscopy (AAS, Australia Spectra-AA200 Varian).

The adsorption capacity, distribution coefficient and removal efficiency of heavy metal ions were determined by the following equations [9, 23]:

$$q = \frac{C_0 - C_e}{\frac{m}{V}} \quad (1)$$

$$K_d = 1,000 \times \frac{C_0 - C_e}{\frac{m}{V} \cdot C_e} \quad (2)$$

$$R (\%) = \frac{C_0 - C_e}{C_0} \times 100 \quad (3)$$

where C_0 and C_e (mg/L) are the initial and equilibrium concentrations of metal ions, V is the volume of solution (L) and m is the weight of adsorbent (g). The distribution coefficient (K_d , mL/g) depicts the concentration of adsorbate onto the solid versus the concentration left in solution.

Characterization

To monitor the variations of functional groups, Fourier transform infrared spectroscopies (FT-IR) of the AMP/PAN nanofiber adsorbent were recorded from 400 to 4,000 cm^{-1} using the German Spectrometer Vector 22 Bruker. The size and morphology of the adsorbent were examined by scanning electron microscopy (SEM, JEOL JSM-6380). Specific surface area was measured by the BET method by the use of USA NOVA-2000 Quantachrome. Total pore volume and pore size were estimated by means of Brett–Joyner–Halenda (BJH) method. The XRD was carried out by Germany STIDY-MP STOE to determine the structure of the AMP/PAN nanofiber adsorbent. The aqueous phase concentration of Cs^+ and other metal ions were distinguished by AAS (Atomic Absorption Spectroscopy, Australia Spectra-AA200 Varian).

Results and discussion

Characterization of the AMP/PAN nanofiber adsorbent

The physicochemical properties of the AMP/PAN nanofiber adsorbent used in this study were measured by BET method and summarized in Table 1. The pore diameter and specific surface area of the adsorbent are important physicochemical properties which show the adsorption efficiency. Based on BJH theory, the average pore diameter of fibers was 2.31 nm with a uniform pore size distribution in the range of 1.8–5.8 nm. The surface area and the pore volume were 31.229 m^2/g and 0.066 cm^3/g , respectively. The synthesized nanofiber adsorbent has very smaller pore diameter (2.31 nm) relative to the AMP/PAN composite (31.41 nm) synthesized by Park et al. [18] but the specific surface area of synthesized composite by Park et al. (32.69 m^2/g) is nearly the same as our result (31.229 m^2/g). The comparison of AMP/PAN nanofiber adsorbent surface area with other PAN-based adsorbents is shown in Table 2. As can be seen, the surface area of our nanofiber adsorbent is in the same range of other adsorbents. The nitrogen adsorption–desorption isotherm of the AMP/PAN nanofiber is shown in Fig. 1a. The volume adsorbed by AMP/PAN nanofiber increased sharply at a relative pressure

Table 1 The physicochemical properties of the AMP/PAN nanofiber adsorbent

Properties	
BET pore volume (cm^3/g)	0.066
BET pore size (nm)	2.310
BET surface area (m^2/g)	31.299

Table 2 Comparison of surface areas (m^2/g) of AMP/PAN nanofiber adsorbent with other adsorbents

Adsorbent	Surface area (m^2/g)	References
Polyacrylonitrile/ferrous chloride	13.8	[24]
Polyacrylonitrile/polyamidoamine (5 %wt/wt)	26.2	[25]
Modified polyacrylonitrile with SiO_2 nanoparticles (5 %wt/wt)	53.2	[26]
AMP/PAN nanofiber adsorbent	31.229	This study

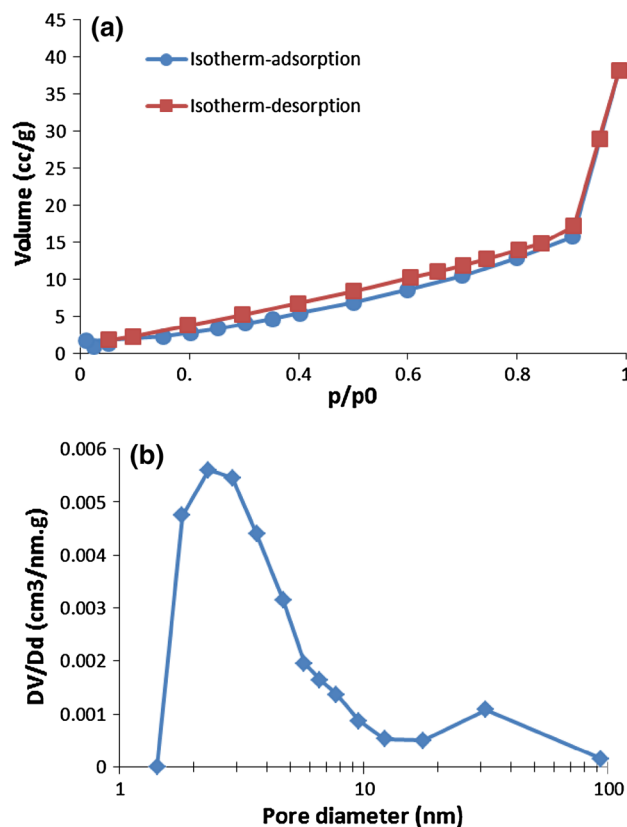


Fig. 1 a The nitrogen adsorption–desorption isotherm and b The pore size distribution of AMP/PAN nanofiber adsorbent

(P/P_0) of about 0.9, depicting capillary condensation of the uniform structure of nanofibers. Also, Fig. 1b shows the pore size distribution of AMP/PAN nanofiber. The value of pore diameter of fibers showed that the surface of AMP/PAN nanofiber was mesoporous.

The XRD pattern of AMP/PAN nanofiber adsorbent is shown in Fig. 2. As can be seen in Fig. 2, there is obvious intensive reflux at $2\theta = 10.7^\circ, 13.1^\circ, 15.1^\circ, 18.6^\circ, 21.5^\circ, 23.75^\circ, 26.5^\circ$ and 28.6° corresponding to 110, 111, 200, 211, 220, 310, 222 and 321 planes manifesting a good

Fig. 2 The XRD pattern of AMP/PAN nanofiber adsorbent

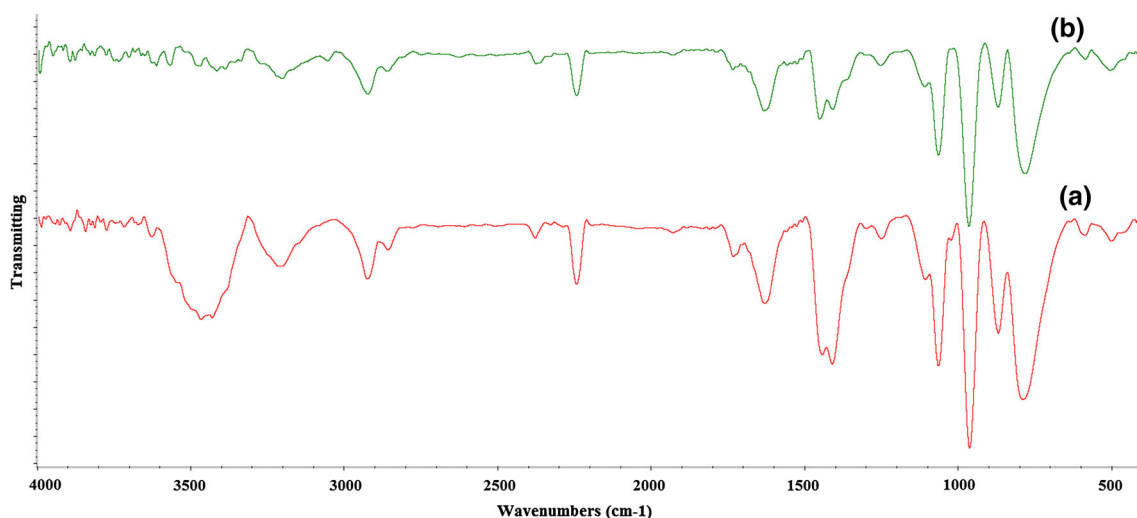
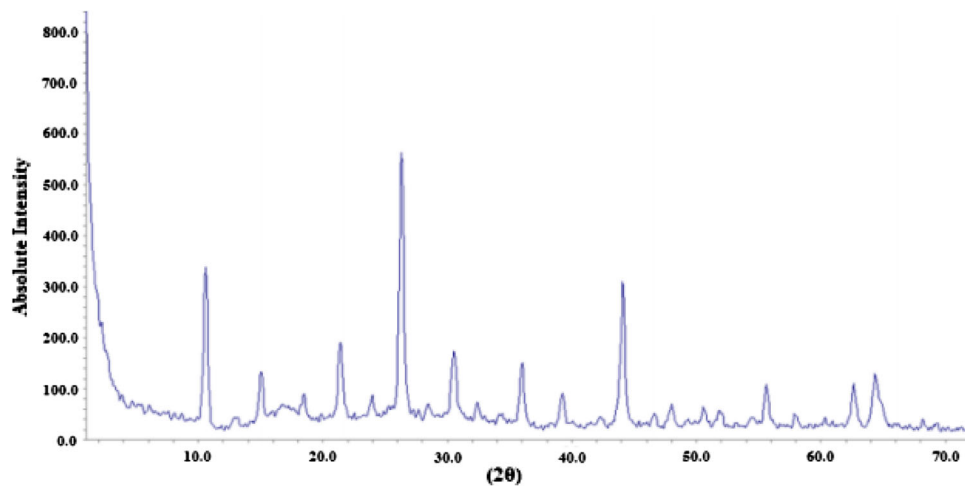


Fig. 3 FT-IR spectra of AMP/PAN nanofiber adsorbent before (a) and after (b) Cs^+ adsorption

agreement with the XRD pattern reported by Nilchi et al. [16] and Sydorchuk et al. [27]. The intensity of peaks implies that the AMP/PAN nanofiber has crystalline structure. Furthermore, comparing the XRD pattern with the mentioned works shows that AMP particles have been loaded on polyacrylonitrile appropriately.

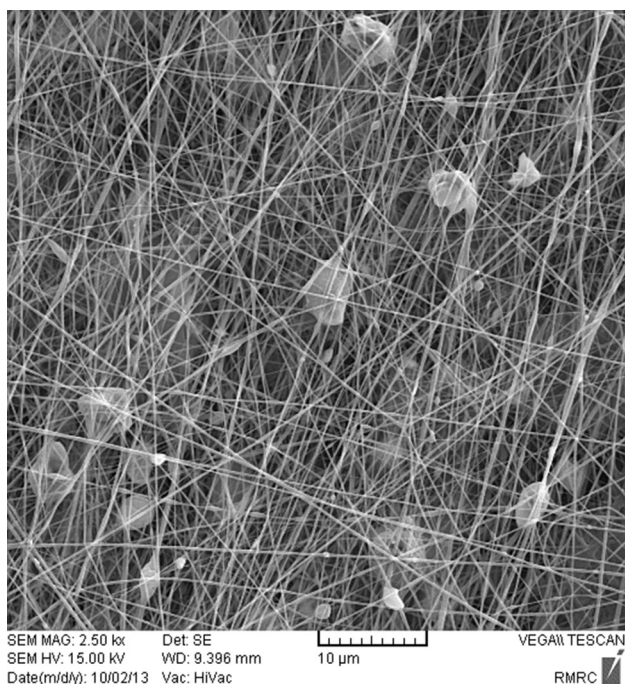
The FT-IR spectroscopic analysis was used for finding the interaction nature between AMP/PAN nanofiber and Cs^+ ions. The spectra of nanofiber samples before and after adsorption process are shown in Fig. 3. Table 3 represents the dominant peaks for them. It can be understood that the bands in the region of $3,310\text{--}3,610\text{ cm}^{-1}$ and $3,117\text{--}3,300$ are related to stretching vibration of --OH group and N--H group, respectively. The peak at $1,408\text{ cm}^{-1}$ corresponds to NH_4^+ and the vibrational bands of P--O , Mo=O and Mo--O--Mo in the AMP are observed from $1,070$, 970 and 870 cm^{-1} to $1,060$, 960 and 860 cm^{-1} , respectively [16,

18]. The peaks at $2,924$, $2,242$, $1,728$ and $1,443\text{ cm}^{-1}$ are attributed to stretching vibration of methylene ($\text{--CH}_2\text{--}$), stretching vibration of nitrile groups (--CN--), stretching vibration of (C=O) and bending vibration of methylene, respectively [28, 29]. By comparing Fig. 3a with Fig. 3b, it is obvious that the adsorption intensities of --OH , NH_4^+ and N--H groups have reduced and the bending vibration of methylene has shifted from $1,443$ to $1,452\text{ cm}^{-1}$. Then, the adsorption between the Cs^+ ions and the --OH , NH_4^+ , N--H and the bending vibration of methylene are identified as the main factors in the adsorption of Cs^+ onto AMP/PAN nanofiber adsorbent.

SEM image of AMP/PAN nanofiber is indicated in Fig. 4. The average diameter of AMP/PAN nanofiber is 190 nm and beads can be seen on the surface of AMP/PAN nanofiber. Obviously, the structure of distribution nanofiber network was dense.

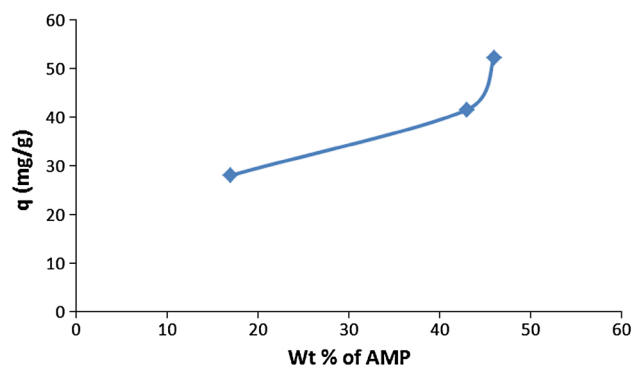
Table 3 Wave number (in cm^{-1}) for the dominant peak from FTIR for before (a) and after (b) Cs^+ adsorption

Functional group	AMP/PAN ^a	AMP/PAN ^b
–OH	3,310–3,610	Reduce intensity
N–H	3,117–3,300	Reduce intensity
Stretching vibration of methylene (–CH ₂ –)	2,924	–
Stretching vibration of nitrile groups (–CN–)	2,242	–
Stretching vibration of (C = O)	1,728	–
Bending vibration of methylene	1,443	1,452
NH ⁴⁺	1,408	Reduce intensity
P–O	1,070–1,060	–
Mo = O	970–960	–
Mo–O–Mo	870–860	–

**Fig. 4** SEM image of AMP/PAN nanofiber adsorbent

Effect of AMP content in AMP/PAN nanofiber adsorbent

To express the effect of AMP weight percentage on the adsorption capacity of Cs^+ ion, AMP/PAN nanofiber adsorbent was prepared in different amounts of AMP (17, 43 and 46 wt% based on the composite weight). The adsorption capacity of Cs^+ ion onto AMP/PAN nanofiber adsorbent is indicated in Fig. 5. As can be seen, the adsorption capacity of AMP/PAN nanofiber increases with rising AMP content up to 46 wt%. This increase is due to a large number of active sites on the adsorbent. In other words, by

**Fig. 5** Effect of the AMP weight percentage on AMP/PAN nanofiber adsorbent for adsorption of Cs^+ ion at 25 °C, pH 5, initial concentration of 100 mg/L and adsorbent concentration of 1 g/L

increasing the weight percentage of AMP in the AMP/PAN adsorbent, the amounts of effective functional groups such as amine increased on the adsorbent. Therefore, AMP (46 %)/PAN nanofiber adsorbent was selected for further experiments.

Effect of solution pH

The pH value of aqueous solution is an important parameter in controlling the adsorption process. The influence of pH is high on adsorption process, especially for monovalent cations, because of competitive adsorption between H^+ ions and metal ions. As can be seen in Fig. 6, there is a low adsorption capacity of Cs^+ in initial pH values, because the active sites of AMP/PAN nanofiber adsorbent are mainly protonated, so they are less available for cations. As pH values increase, the available sites for cations and the adsorption capacity of Cs^+ by AMP/PAN nanofiber adsorbent reach the maximum at pH 5. Moreover, it is obvious that with rising pH value, the adsorption capacity decreases; this phenomenon can be due to the formation of stable Cs^+ complexes. So, the pH 5 is considered optimum pH for further experiments.

Effect of adsorbent concentration

The effect of AMP/PAN nanofiber adsorbent concentration (g/L) on the removal efficiency and adsorption capacity was studied for Cs^+ ions at pH 5.0. As shown in Fig. 7, the adsorption capacity first increased to reach maximum value at adsorbent concentration of 1 (g/L) and then reduced with increasing AMP/PAN nanofiber adsorbent concentration. On the other hand, the removal efficiency (R %) increased as AMP/PAN nanofiber adsorbent concentration enhanced. The efficiency sharply increased with increasing AMP/PAN nanofiber adsorbent concentration up to 3 g/L. It was found that the efficiencies were 97 and 98 % in 3 and 4 g/L

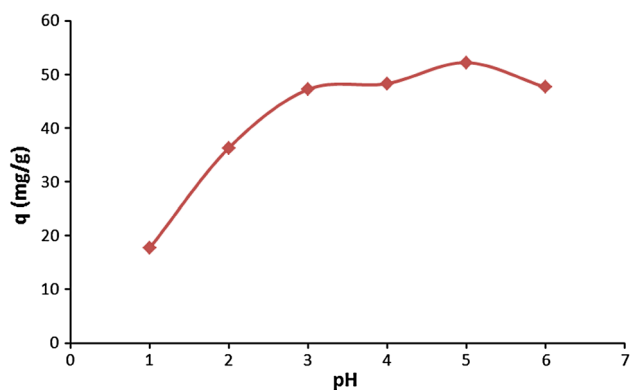


Fig. 6 Effect of pH on adsorption capacity of Cs^+ ion at 25 °C, initial concentration of 100 mg/L and adsorbent concentration of 1 g/L

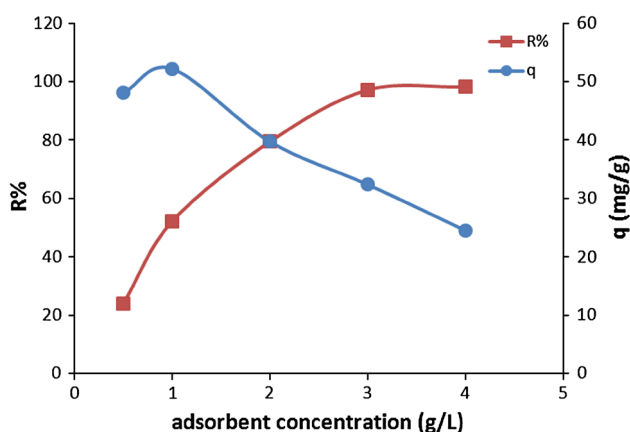


Fig. 7 Effect of adsorbent concentration on removal efficiency and adsorption capacity of Cs^+ ion at 25 °C, pH 5 and initial concentration of 100 mg/L

of nanofiber adsorbent concentrations, respectively. By increasing the concentration of nanofiber and available adsorption sites, access of Cs^+ ions to adsorption sites on the surface of AMP/PAN nanofiber adsorbent increased. The process has resulted in increasing Cs^+ removal efficiency.

Effect of contact time

As expected and was indicated in Fig. 8, the adsorption of Cs^+ by AMP/PAN nanofiber initially went up rapidly within 1 h (about 83 %) and then slowly reached the saturation at about 5 h. The Cs^+ ions initially occupied many of the active sites on the adsorbent surface in a random manner, as a result of which the rate of adsorption was faster. With time, the rate of adsorption slowed down and reached a constant value because of surface saturation, and repulsive forces among adsorbed Cs^+ ions and those presented in the solution. No significant change in

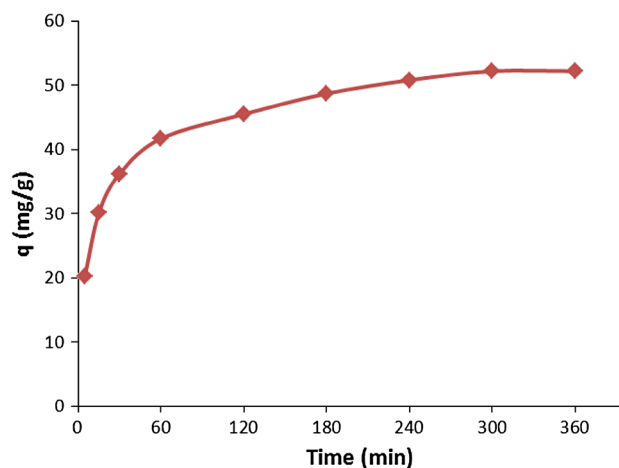


Fig. 8 Effect of contact time on adsorption capacity of Cs^+ ion at 25 °C, pH 5, initial concentration of 100 mg/L and adsorbent concentration of 1 g/L

adsorption percentage was observed up to 5 h. Based on these results, a shaking time of 5 h was found to be suitable for all equilibrium adsorption experiments.

Kinetic models

The adsorption kinetic prepared valuable information to find out the reaction pathways and the mechanism of an adsorption reaction. The four kinetic models were tested in this investigation.

The pseudo-first-order and pseudo-second-order kinetic models were used to predict the Cs^+ adsorption kinetic. The pseudo-first-order model supposes that the changing rate of occupation of adsorption sites is directly proportional to the number of unoccupied sites. The linear form is expressed as [30]:

$$\ln(q_e - q_t) = \ln q_e - k_1 t \quad (4)$$

The pseudo-second-order assumes that the rate of occupation of adsorption sites is proportional to the square of the number of unoccupied sites and the overall rate of adsorption process is controlled by the chemisorptions. The linear form is expressed as [31]:

$$\frac{t}{q_t} = \frac{1}{q_e} t + \frac{1}{k_2 q_e^2} \quad (5)$$

where q_t and q_e are the amounts of Cs^+ adsorbed (mg/g) at time t and equilibrium time, respectively and k_1 (min^{-1}) and k_2 ($\text{g}/\text{mg}\cdot\text{min}$) are the pseudo-first-order and pseudo-second-order rate constants.

Elovich's kinetic equation is based on the adsorption capacity. It is mostly used to denote the kinetics of adsorption and properly explain the dominant chemical adsorption on highly heterogeneous adsorbents. The Elovich linear form is expressed as [32]:

$$q_t = \left(\frac{1}{\beta}\right) \ln(\alpha\beta) + \left(\frac{1}{\beta}\right) \ln t \tag{6}$$

where α is Elovich coefficient which represents the initial adsorption rate (mg/g.min) and β is a constant related to the extent of surface coverage and activation energy for chemisorption (g/mg).

The intraparticle diffusion model is another kinetic model, which assumes that the overall rate of transfer of Cs^+ ions from their aqueous media to the active sites on the adsorbent is controlled by intraparticle diffusion of Cs^+ ions to the pores of adsorbent. The linear form of equation is obtained from [33]:

$$q_t = k_p t^{0.5} + C \tag{7}$$

The rate parameter k_p is intraparticle diffusion rate constant (mg/g.min^{1/2}) and C is related to the boundary layer thickness that can be evaluated from plot of q versus $t^{0.5}$. The kinetic data of Cs^+ adsorption onto AMP/PAN nanofiber adsorbent was predicted by kinetic models. The corresponding fitting parameters are summarized in Table 4.

In this study, the residual root mean square errors (RMSE) and the correlation coefficients (R^2) of models were applied to measure the quality of fit. RMSE can be expressed as [23]:

$$\text{RMSE} = \sqrt{\left(\frac{1}{n-2}\right) \sum_{i=1}^n (q_{i,\text{exp}} - q_{i,\text{cal}})^2} \tag{8}$$

where $q_{i,\text{exp}}$ and $q_{i,\text{cal}}$ are the experimental and calculated values of the adsorption capacity, respectively and n is the number of data points. A smaller RMSE value indicates a better curve fitting.

Hence, according to the RMSE and R^2 values, the experimental results best fitted the pseudo-second-order rate equation and resulted in a linear plot with high regression coefficient (R^2) and low RMSE values equal to 0.9996 and 0.051, respectively. Also, the predicted adsorption capacity was equal to 54.05 mg/g that was close to the experimental adsorption capacity (52.2 mg/g). This illustrates that the adsorption of Cs^+ ion on AMP/PAN nanofiber adsorbent follows the pseudo-second-order kinetics and the overall rate of adsorption process is controlled by the chemisorption step.

Effect of initial concentration and temperature

The change in adsorption behavior of AMP/PAN nanofiber adsorbent with different Cs^+ ion concentrations from 10 to 100 mg/L at various temperatures (25–45 °C) is illustrated in Fig. 9. As can be seen, the adsorption capacity of AMP/

Table 4 The parameters of kinetic models for Cs^+ adsorption onto AMP/PAN nanofiber adsorbent

Pseudo-first-order model			
k_1 (min ⁻¹)	q_e (mg g ⁻¹)	R^2	RMSE
0.0,294	62.68	0.8982	1.39
Pseudo-second-order model			
k_2 (g mg ⁻¹ min ⁻¹)	q_e (mg g ⁻¹)	R^2	RMSE
0.0014	54.05	0.9996	0.051
Elovich model			
α	β	R^2	RMSE
26.24	0.1298	0.9794	1.77
Intraparticle diffusion model			
k_p (mg g ⁻¹ min ^{-1/2})	C	R^2	RMSE
1.739	24.25	0.8450	4.85

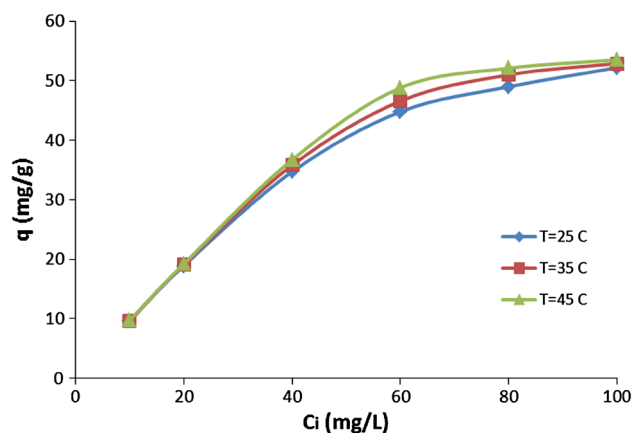


Fig. 9 Effect of initial concentration and temperature on capacity adsorption of Cs^+ ion in 25 °C, pH 5 and adsorbent concentration of 1 g/L

PAN nanofiber adsorbent increases with enhancing initial concentration of Cs^+ ion. This uptrend may be related to the increase in the initial ion concentration preparing a greater driving force to prevail the entire mass transfer resistance between the solid and liquid phases, thus resulting in higher Cs^+ ion adsorption. Also, as can be seen in Fig. 9, by increasing temperature from 25 to 45 °C the Cs^+ adsorption capacity increases. This increase can be due to the acceleration of some slow adsorption steps or due to the creation of new vacant active sites on the adsorbent surface.

Adsorption isotherm models

The relation between the adsorbed Cs^+ ions on the solid surface and those remaining in solution is expressed by isotherm models. Three mostly recognized adsorption isotherms, namely Langmuir model, Freundlich model and Dubinin and Radushkevich model were used to investigate the equilibrium data of Cs^+ adsorption onto AMP/PAN nanofiber adsorbent.

The Langmuir isotherm is valid for monolayer adsorption without interaction between the adsorbed molecules onto a surface including a finite number of identical sites [13]. The linear form is described by the following equation:

$$\frac{C_e}{q_e} = \frac{1}{q_{\text{mL}} \cdot b_L} + \frac{1}{q_{\text{mL}}} C_e \quad (9)$$

where q_{mL} is the maximum adsorption capacity (mg/g) and b_L is the constant related to the free energy of adsorption (L/mg).

The favorability of Cs^+ adsorption onto AMP/PAN nanofiber adsorbent can be measured from dimensionless constant called separation factor, R_L .

$$R_L = \frac{1}{1 + b_L C_0} \quad (10)$$

where C_0 is the highest initial Cs^+ ion concentration (mg/L). The value of R_L shows the unfavorable ($R_L > 1$), linear ($R_L = 1$), favorable ($0 < R_L < 1$) and irreversible ($R_L = 0$) types of the adsorption isotherm [31].

Freundlich isotherm is widely applied to explain multilayer adsorption associated with adsorption on heterogeneous surfaces without uniform distribution of adsorption heat and affinity; although, it is valid for adsorption data over a restricted range of concentrations. The linear form is represented below [30]:

$$\ln q_e = \ln K_f + \frac{1}{n_f} \ln C_e \quad (11)$$

where $1/n_f$ and K_f are the isotherm parameters of adsorption intensity and adsorption capacity (mg/g) (L mg^{-1})^{1/n}, respectively. The Freundlich exponent, $1/n_f$, is a measure of the deviation from linearity of the adsorption. If the $1/n_f$ value equals to unity, the adsorption is linear and between 0 and 1 showing that the adsorption is favorable [34].

A further equation has been considered by Dubinin and Radushkevich (D–R) for the analysis of isotherms, which is based on Polanyi's adsorption potential theory and Dubinin's micropore filling theory. The linearized D–R isotherm is expressed as follows [34]:

$$\ln q_e = \ln q_{\text{mD}} - \beta \varepsilon^2 \quad (12)$$

where β (mol^2/J^2) is the activity coefficient related to adsorption mean free energy and ε (J/mol) is the Polanyi potential which can be determined from equation:

$$\varepsilon = RT \ln \left(1 + \frac{1}{C_e} \right) \quad (13)$$

where q_{mD} (mmol/g) is the theoretical maximum adsorption capacity, R (J/mol.K) is the gas constant and T (K) is the absolute temperature.

On the other hand, the activity coefficient is related to the mean free energy of adsorption per mole of adsorbate (E , J/mol), when it is transferred to the surface of the solid from infinity in the solution, according to the following equation:

$$E = \frac{1}{\sqrt{2\beta}} \quad (14)$$

The obtained E values prepare useful information about adsorption mechanism, i.e., it is a physical or chemical process. A value between 8 and 16 kJ/mol indicates that the adsorption process takes place chemically, while for the values less than 8 kJ/mol, the adsorption process is of a physical nature [34].

The calculated model parameters are tabulated in Table 5. Among these adsorption models, the best correlations are observed in the light of Langmuir isotherm model with $R^2 > 0.9987$ and RMSE < 0.014 . The Langmuir isotherm which fits the experimental data very well may be due to the homogenous distribution of active sites on AMP/PAN nanofiber adsorbent. Table 5 shows that the maximum adsorption capacity based on the Langmuir model increases from 54.05 to 55.25 mg/g with a rise in temperature from 25 to 45 °C. The comparison of Langmuir adsorption capacity of Cs^+ by AMP/PAN nanofiber adsorbent at room temperature (25 °C) with other adsorbents mentioned in the literature is shown in Table 6. It can be concluded from the reported Langmuir adsorption capacities that the Langmuir capacity of AMP/PAN nanofiber adsorbent is in the range of the results obtained by other researchers. Also, as can be seen in Table 5, the values of R_L are between 0 and 1 indicating favorable adsorption of Cs^+ ions onto AMP/PAN nanofiber adsorbent. It is observed in Table 5 that the $1/n_f$ values are between 0 and 1 at all temperatures indicating again that the adsorption of Cs^+ onto the AMP/PAN is favorable under studied conditions. Also, the calculated E values are close to 8 kJ/mol indicating that the Cs^+ adsorption onto AMP/PAN nanofiber adsorbent occurs via chemical adsorption.

Table 5 The parameters of isotherm models for Cs⁺ adsorption onto AMP/PAN nanofiber adsorbent

Temp. (°C)	Langmuir				
	<i>q_{mL}</i> (mg/g)	<i>b_L</i> (L/mg)	<i>R_L</i>	<i>R</i> ²	RMSE
25	54.05	0.3979	0.025	0.9987	0.014
35	54.64	0.5185	0.019	0.9997	0.007
45	55.25	0.6728	0.015	0.9999	0.003
Temp. (°C)	Freundlich				
	1/ <i>n_f</i>	<i>K_f</i> (mg/g) (L.mg ⁻¹) ^{1/<i>n</i>}	<i>R</i> ²	RMSE	
25	0.342	16.14	0.9417	0.181	
35	0.332	17.6	0.927	0.205	
45	0.325	18.92	0.9062	0.236	
Temp. (°C)	D–R				
	<i>q_{mD}</i> (mmol/g)	<i>β</i> (×10 ⁸) (mol ² /J ²)	<i>E</i> (kJ/mol)	<i>R</i> ²	RMSE
25	0.439	0.84	7.7	0.9955	0.050
35	0.458	0.75	8.2	0.9921	0.067
45	0.477	0.68	8.6	0.9865	0.090

Table 6 Comparison of Langmuir adsorption capacity (mg/g) of AMP/PAN nanofiber adsorbent for Cs⁺ adsorption with other adsorbents mentioned in the literature at room temperature (25 °C)

Adsorbent	<i>q_{mL}</i> (mg/g)	References
Ammonium molybdophosphate–calcium alginate composite	90.38	[4]
Agricultural residue-Walnut shell	4.94	[6]
Polyaniline titanotungstate	227.79	[7]
Sericite	6.68	[9]
Zeolite A	207.47	[10]
Prussian blue caged in alginate/calcium beads	131.57	[13]
Ammonium molybdophosphate–calcium alginate composite	61.45	[15]
Polyacrylonitrile based manganese dioxide composite	321.64	[16]
AMP/PAN granule	81.07	[18]
AMP/PAN nanofiber adsorbent	52.2	This study

Adsorption thermodynamic

It is essential to study the effect of temperature on Cs⁺ adsorption by AMP/PAN nanofiber adsorbent. The equilibrium adsorption constant (*K_C*) depending on the temperature was applied to distinguish the values of Δ*G*[°], Δ*H*[°] and Δ*S*[°]. The values of *K_C* were calculated from the following equation [23]:

$$K_C = \lim_{C_e \rightarrow 0} \frac{C_{es}}{C_{el}} \tag{15}$$

where *C_{el}* (mg/L) and *C_{es}* are the equilibrium concentrations of Cs⁺ ions in liquid and solid phases, respectively. According to the plot of the experimental data of $\frac{C_{es}}{C_{el}}$ versus *C_{el}* (figure is not illustrated), the values of *K_C* at different temperatures (25, 35 and 45 °C) are evaluated. The adsorption standard free energy (Δ*G*[°]) is obtained from [23]:

$$\Delta G^\circ = -RT \ln K_C \tag{16}$$

The thermodynamic parameters Δ*H*[°] and Δ*S*[°] for the adsorption process are calculated from the slopes and intercepts of the linear variation of ln *K_C* versus 1/*T* by the following equation [23]:

$$\ln K_C = \frac{\Delta S}{R} - \left(\frac{\Delta H}{R} \right) \frac{1}{T} \tag{17}$$

The thermodynamic parameters of Cs⁺ adsorption onto AMP/PAN nanofiber adsorbent are shown in Table 7. The positive value of Δ*H*[°] indicates an endothermic adsorption process. Also, an increase in negative Δ*G*[°] values with rising the temperature suggests that the adsorption process is spontaneous and favorable at higher temperatures. Positive magnitudes of entropy show that the randomness at the solid–liquid interface during the adsorption process increases.

The capability adsorption for other metal ions

Real wastewater contains many types of metal ions in addition to Cs⁺ ions. So besides Cs⁺ ion, the AMP/PAN nanofiber adsorbent was also applied to adsorb Co²⁺, Sr²⁺, Mg⁺ and Ca²⁺ metal ions from aqueous solutions. The batch equilibrium experiments were performed in single metal ion systems under conditions of initial metal ions of 100 mg/L, adsorbent concentration of 1 g/L, 25 °C and pH 5. The results are shown in Table 8. The adsorption capacity of Co²⁺, Sr²⁺, Mg⁺ and Ca²⁺ ions onto the AMP/PAN nanofiber adsorbent were 8.6, 0.9, 7.5 and 3.0 mg/g, respectively. Compared with the adsorption capacity for Cs⁺ ions (52.2 mg/g), the adsorption affinity of metal ions onto the adsorbent was in the order of Cs⁺ > Co²⁺ > Mg²⁺ > Ca²⁺ > Sr²⁺. Also, for investigation of Cs⁺ preferential adsorption by AMP/PAN nanofiber adsorbent, the Cs⁺ ion separation factor α can be evaluated as [7]:

$$\alpha = \frac{K_d(Cs)}{K_d(i)} \tag{18}$$

where *K_d* (*i*) is the distribution coefficient for component *i*. According to this equation, α > 1 shows the preference of adsorbent toward component *i* against other components

Table 7 The thermodynamic parameters for Cs⁺ adsorption onto AMP/PAN nanofiber adsorbent

K_C			ΔH° (kJ/mol)	ΔS° (kJ/mol K)	ΔG° (kJ/mol)		
25 °C	35 °C	45 °C			25 °C	35 °C	45 °C
27.2	31.8	38.9	14.08	0.075	-8.18	-8.92	-9.67

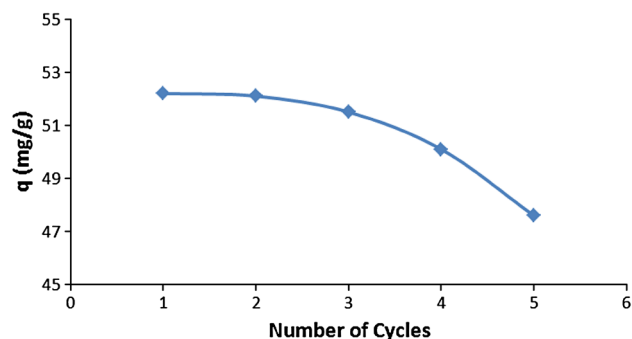
Table 8 The adsorbent capability for metal ions adsorption

Metal ion	q_e (mg/g)	K_d (mL/g)	α_B^{Cs}
Cs	52.2	1,092.05	1
Co	8.6	93.94	11.6
Sr	0.9	9.07	120.3
Mg	7.5	80.87	13.5
Ca	3.0	31.11	35.1

and higher amounts of it prove proper selectivity of adsorbent for the component *i*. The effect of the size and charge of the metal ions on K_d values was seen on AMP/PAN nanofiber adsorbent. The K_d values indicate a reducing trend in order of Cs⁺ >>> Co²⁺ > Mg²⁺ > Ca²⁺ > Sr²⁺. The effective removal of Cs⁺ shows not only the chemical adsorption properties but also the metal ion-sieve characteristic according to the pore diameter of fibers. Metal ions with smaller unhydrated radii easily occupy the pores of the fibers, which results in higher adsorption. Moreover, the high K_d value for Cs⁺ verifies crystalline structure for adsorption and the appropriate AMP particles loaded on AMP/PAN nanofiber adsorbent. The results are illustrated in Table 8. As can be seen, the Cs⁺ separation factors related to Co²⁺, Mg²⁺, Ca²⁺ and Sr²⁺ are 11.6, 13.5, 35.1 and 120.3, respectively. The separation factor values indicated that AMP/PAN nanofiber adsorbent could selectively separate Cs⁺ ions from other metal ions. Hence, AMP/PAN nanofiber adsorbent was more sensitive to Cs⁺ ions than other metal ions, which were consistent with the other reported results [18, 35].

Regeneration of AMP/PAN nanofiber adsorbent

A good adsorbent, in addition to its high adsorption capacity must also exhibit good regeneration ability for multiple uses. In this study, 1 M NH₄Cl solution [16, 36] was selected for regenerating process at a temperature of 25 °C, contact time of 24 h and adsorbent concentration of 1 g/L and initial Cs⁺ ion concentration of 100 mg/L. The reusability of the adsorbent was estimated in five adsorption–desorption cycles, the results of which are shown in Fig. 10. It can be seen that the adsorption capacity of AMP/PAN nanofiber reduced from 52.2 to 47.6 mg/g (about

**Fig. 10** Five cycles of Cs⁺ adsorption–desorption with 1 M NH₄Cl

9 %) after five cycles of adsorption–desorption, respectively. This indicates that the AMP/PAN nanofiber adsorbent can be reused frequently without almost any significant loss in adsorption performance and can be a good material for removal and recovery of Cs⁺ from aqueous solution.

Conclusion

In this investigation, a novel AMP/PAN nanofiber adsorbent for Cs⁺ removal from aqueous solution was prepared by electrospinning method and characterized by FTIR, BET, XRD and SEM analyses. FTIR analysis demonstrated the involvement of different functional groups of mainly hydroxyl, amine and methylene. The effect of AMP weight percentage in the AMP/PAN nanofiber adsorbent showed that Cs⁺ adsorption capacity increased with an increase in AMP weight percentage. The effect of pH on adsorption capacity of Cs⁺ onto AMP/PAN nanofiber adsorbent depicted that this adsorbent could be effectively applied within the pH range of 3–6. Adsorption kinetics was vividly depicted by the pseudo-second-order ($R^2 = 0.9996$ and RMSE = 0.051) with an equilibrium time of 5 h. Three isotherm models were used for analysis of equilibrium data and the best correlation was obtained by Langmuir model. The results showed that the maximum adsorption capacity based on the Langmuir model increased from 54.05 to 55.25 mg/g with an increase in temperature from 25 to 45 °C. The negative value of ΔG° and the positive value of ΔH° confirm the spontaneous and

the endothermic nature of the adsorption process. The adsorption capacity of Cs^+ , Co^{2+} , Mg^{2+} , Sr^{2+} and Ca^{2+} ions by the AMP/PAN nanofiber adsorbent was in the order: $\text{Cs}^+ > \text{Co}^{2+} > \text{Mg}^{2+} > \text{Ca}^{2+} > \text{Sr}^{2+}$. The separation factor values indicated that AMP/PAN nanofiber adsorbent could selectively separate Cs^+ ions from other metal ions. The results from XRD and BET analyses for crystalline structure, pore diameter and specific surface area proved high adsorption and selectivity. The Cs^+ adsorption–desorption cycles which were consistently repeated by using NH_4Cl solution and indicated the feasibility of AMP/PAN nanofiber adsorbent for Cs^+ removal.

Acknowledgments Hereby, the authors wish to acknowledge the Research Laboratory of Multi-Component Separation in the School of Chemical Engineering of University of Tehran for supporting this research.

References

1. Yusof NNM, Kikuchi Y, Kobayashi T (2014) Predominant hosting lead(II) in ternary mixtures of heavy metal ions by a novel of diethylaminomethyl-calix [4] resorcinarene. *Int J Environ Sci Technol* 11:1063–1072
2. Mao Y, Hu H, Yan Y (2011) Biosorption of cesium (I) from aqueous solution by a novel exopolymers secreted from *Pseudomonas fluorescens* C-2: equilibrium and kinetic studies. *J Environ Sci* 23(7):1104–1112
3. Nagy P, Vajda N, Sziklai-László I, Kovács-Széles É, Simonits A (2014) Determination of ^{137}Cs in nuclear power plant wastes by ICP-MS and k 0-NAA. *J Radioanal Nucl Chem* 300(2):615–627
4. Xiushen Y, Wu Z, Li W, Liu H, Li Q, Qing B, Guo M, Ge F (2009) Rubidium and cesium ion adsorption by an ammonium molybdophosphate–calcium alginate composite adsorbent. *Colloid Surf A* 342:76–83
5. Karamanis D, Assimakopoulos PA (2007) Efficiency of aluminum-pillared montmorillonite on the removal of cesium and copper from aqueous solutions. *Water Res* 41:1897–1906
6. Dahu D, Zhao Y, Yang S, Shi W, Zhang Z, Lei Z, Yang Y (2013) Adsorption of cesium from aqueous solution using agricultural residue-walnut shell: equilibrium, kinetic and thermodynamic modeling studies. *Water Res* 47:2563–2571
7. El-Naggar IM, Zakaria ES, Ali IM, Khalil M, El-Shahat MF (2012) Chemical studies on polyaniline titanotungstate and its uses to reduction cesium from solutions and polluted milk. *J Environ Radioact* 112:108–117
8. Deng PY, Liu W, Zeng BQ, Qiu YK, Li LS (2013) Sorption of heavy metals from aqueous solution by dehydrated powders of aquatic plants. *Int J Environ Sci Technol* 10:559–566
9. Kim J, Lee S, Jeon Ch, (2013). Adsorption characteristics of sericite for cesium ions from an aqueous solution. *Chem Eng Res Des*, <http://dx.doi.org/10.1016/j.cherd.2013.07.020>
10. El-Kamash AM (2008) Evaluation of zeolite A for the sorptive removal of Cs^+ and Sr^{2+} ions from aqueous solutions using batch and fixed bed column operations. *J Hazard Mater* 151:432–445
11. Wu S, Li F, Wang H, Fu L, Zhang B, Li G (2010) Effects of poly(vinyl alcohol)(PVA) content on preparation of novel thiol-functionalized mesoporous PVA/SiO₂ composite nanofiber membranes and their application for adsorption of heavy metal ions from aqueous solution. *Polymer* 51:6203–6211
12. Justi KC, Fávere VT, Laranjeira M, Neves A, Peralta RA (2005) Kinetics and equilibrium adsorption of Cu (II), Cd (II), and Ni (II) ions by chitosan functionalized with 2[-bis-(pyridyl-methyl)aminomethyl]-4-methyl-6-formylphenol. *J Colloid Interface Sci* 291:369–374
13. Vipin AK, Hu B, Fugetsu B (2013) Prussian blue caged in alginate/calcium beads as adsorbents for removal of cesium ions from contaminated water. *J Hazard Mater* 258–259:93–101
14. Raouf MW (2004) Potassium hexacyanocobalt ferrate and ammonium molybdophosphate adsorption bags for the removal of ^{137}Cs from aqueous solutions and a simulated waste. *J Chem Technol Biotechnol* 79:22–29
15. Mimura H, Saito M, Akiba K, Onodera Y (2001) Selective uptake of cesium by ammonium molybdophosphate (AMP)–calcium alginate composites. *J Nucl Sci Technol* 38:872–878
16. Nilchi A, Saberi R, Rasoul Garmarodi S, Bagheri A (2012) Evaluation of PAN-based manganese dioxide composite for the sorptive removal of cesium-137 from aqueous solutions. *Appl Radiat Isot* 70:369–374
17. Šebesta F, Štefula V (1990) Composite ion exchanger with ammonium molybdophosphate and its properties. *J Radioanal Nucl Chem* 140:15–21
18. Park Y, Lee YC, Shin WS, Choi SJ (2010) Removal of cobalt, strontium and cesium from radioactive laundry wastewater by ammonium molybdophosphate–polyacrylonitrile (AMP–PAN). *Chem Eng J* 162:685–695
19. Taha AA, Qiao J, Li F, Zhang B (2012) Preparation and application of amino functionalized mesoporous nanofiber membrane via electrospinning for adsorption of Cr^{3+} from aqueous solution. *J Environ Sci* 24:610–616
20. Min M, Shen L, Hong G, Zhu M, Zhang Y, Wang X, Chen Y, Hsiao BS (2012) Micro-nano structure poly (ether sulfones)/poly (ethyleneimine) nanofibrous affinity membranes for adsorption of anionic dyes and heavy metal ions in aqueous solution. *Chem Eng J* 197:88–100
21. Sang Y, Gu Q, Sun T, Li F, Liang C (2008) Filtration by a novel nanofiber membrane and alumina adsorption to remove copper (II) from groundwater. *J Hazard Mater* 153:860–866
22. Chronakis IS (2005) Novel nanocomposites and nanoceramics based on polymer nanofibers using electrospinning process—a review. *J Mater Process Technol* 167:283–293
23. Abbasizadeh S, Keshtkar AR, Mousavian MA, (2013). Sorption of heavy metal ions from aqueous solution by a novel cast PVA/TiO₂ nanohybrid adsorbent functionalized with amine groups. *J Ind Eng Chem*, <http://dx.doi.org/10.1016/j.jiec.2013.08.013>
24. Zhou S, Liu F, Zhang Q, Chen BY, Lin CJ, Chang CT (2015) Preparation of polyacrylonitrile/ferrous chloride composite nanofibers by electrospinning for efficient reduction of Cr(VI). *J Nanosci Nanotechnol* 15(8):5823–5832
25. Almasian A, Olya ME, Mahmoodi NM (2015) Synthesis of polyacrylonitrile/polyamidoamine composite nanofibers using electrospinning technique and their dye removal capacity. *J Taiwan Inst Chem Eng* 1–10
26. Dastbaz A, Keshtkar AR (2014) Adsorption of Th^{4+} , U^{6+} , Cd^{2+} , and Ni^{2+} from aqueous solution by a novel modified polyacrylonitrile composite nanofiber adsorbent prepared by electrospinning. *Appl Surf Sci* 293:336–344
27. Sydorochuk V, Khalameida S, Skubiszewska-Zięba J, Leboda R (2011) Synthesis and structure of AMP/oxide support. *J Therm Anal Calorim* 103:257–265
28. Neghlani PK, Rafizadeh M, Taromi FA (2011) Preparation of aminated-polyacrylonitrile nanofiber membranes for the adsorption of metal ions: comparison with microfibers. *J Hazard Mater* 186:182–189

29. Lee S, Kim J, Ku BC, Kim J, Joh HI (2012) Structural evolution of polyacrylonitrile fibers in stabilization and carbonization. *Adv Chem Eng Sci* 2:275–282
30. Long H, Wu P, Zhu N (2013) Evaluation of Cs⁺ removal from aqueous solution by adsorption on ethylamine-modified montmorillonite. *Chem Eng J* 225:237–244
31. Faghihian H, Moayed M, Firooz A, Iravani M (2013) Synthesis of a novel magnetic zeolite nanocomposite for removal of Cs⁺ and Sr²⁺ from aqueous solution: kinetic, equilibrium and thermodynamic studies. *J Colloid Interface Sci* 393:445–451
32. Sheha RR, El-Khouly SH (2013) Adsorption and diffusion of cesium ions in zirconium (IV) iodomolybdate exchanger. *Chem Eng Res Des* 91:942–954
33. Lv K, Xiong LP, Luo YM (2013) Ion exchange properties of cesium ion sieve based on zirconium molybdopyrophosphate. *Colloid Surf A* 433:37–46
34. Hasan HA, Abdullah SRS, Kofli NT, Kamarudin SK (2012) Isotherm equilibria of Mn²⁺ biosorption in drinking water treatment by locally isolated *Bacillus* species and sewage activated sludge. *J Environ Manag* 111:34–43
35. Tranter TJ, Vereshchagina TA, Utgikar V (2009) An inorganic microsphere composite for the selective removal of ¹³⁷cesium from acidic nuclear waste solutions. 1: equilibrium capacity and kinetic properties of the sorbent. *Solvent Extr Ion Exch* 27:199–218
36. Nilchi A, Saberi R, Moradi M, Azizpour H, Zarghami R (2012) Evaluation of AMP–PAN composite for adsorption of Cs⁺ ions from aqueous solution using batch and fixed bed operations. *J Radioanal Nucl Chem* 292:609–617